JACS
JOURNAL OF THE AMERICAN CHEMICAL SOCIETY

Article

pubs.acs.org/JACS

Studying the Conformation of a Silaffin-Derived Pentalysine Peptide Embedded in Bioinspired Silica using Solution and Dynamic Nuclear Polarization Magic-Angle Spinning NMR

Yasmin Geiger,[†] Hugo E. Gottlieb,[†] Ümit Akbey,[‡,§,⊥] Hartmut Oschkinat,[‡] and Gil Goobes*[,†]

[†]Department of Chemistry, Bar Ilan University, Ramat Gan 52900, Israel

[‡]Leibniz Institute für Molekulare Pharmakologie (FMP), NMR Supported Structural Biology, Robert-Roessle-Str. 10, Berlin 13125, Germany

Supporting Information

ABSTRACT: Smart materials are created in nature at interfaces between biomolecules and solid materials. The ability to probe the structure of functional peptides that engineer biogenic materials at this heterogeneous setting can be facilitated tremendously by use of DNP-enhanced solid-state NMR spectroscopy. This sensitive NMR technique allows simple and quick measurements, often without the need for isotope enrichment. Here, it is used to characterize a pentalysine peptide, derived from a diatom's silaffin protein. The peptide accelerates the formation of bioinspired silica and gets embedded inside the material as it is formed. Two-dimensional DNP MAS NMR of the silica-bound peptide and solution NMR of the free peptide are used to derive its secondary structure in the two states and to pinpoint some subtle conformational changes that the peptide undergoes in order to adapt to the silica environment. In addition, interactions between abundant lysine residues and silica surface are identified, and proximity of other side chains to silica and to neighboring peptide molecules is discussed.

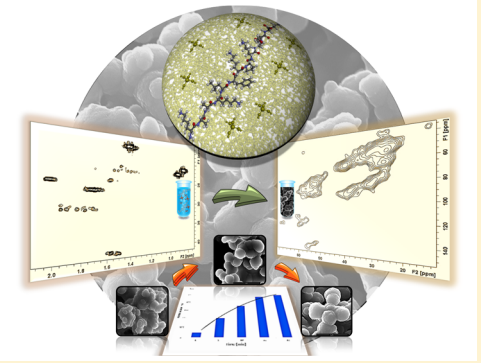

INTRODUCTION

Design of new materials is inspired by the sculpting capabilities of organisms. Diatoms, for instance, produce silica cell walls with intricate and divergent structural designs.[1] These silica structures called frustules, with nanometer to micron size pores, were recently employed for fabrication of functional titania and silicon replicas for nanoelectronics, catalysis and biotechnology applications.[2−6]

The biological processes underlying the formation of silica structures in diatoms were also extensively investigated.[7−10] Several families of proteins, active in precipitation of the silicon oxide material, were found. In particular, silaffin proteins were shown to have a key role in catalysis of silicic acid condensation into silica inside special silica deposition vesicles (SDV) in the diatom cell. Silaffins are also thought to be actively involved in regulation of frustule shape by assembling with long chain polyamines[8,11,12] into templates on which silica is polymerized.

Though different silaffins have generally low-sequence homology, repeat segments with high affinity to silica were found that are rich in lysine and serine residues.[13−15] These residues enable silaffins and peptides derived from them to induce silica precipitation in vitro.[16−20] One such peptide is R5, derived from the silaffin protein Sil1 of *Cylindrotheca fusiformis*. R5 catalyzed silica precipitation into spherical nanoparticles in vitro under neutral pH conditions despite lacking phosphates on its serine residues, common in the native silaffin.[17,19,20]

Poulsen and Kröger[13] recently identified common repeats in silaffins with the following sequence, KxxKxxKyKxxK, (where y represents 1−3 residues depending on the domain in the protein). These lysine-rich segments, termed pentalysine clusters, showed high affinity to silica cell wall in diatoms.[13] In an extensive mutation study of T6 and T7, pentalysine domains from another silaffin (Sil3) in *Thalassiosira pseudonana*, the role of pentalysine sequences in the integrity of frustule structure was demonstrated.[13] The impact of the lysines was shown to be more than a simple cumulative effect of the positive charges and hydrogen bonds they can form.[13,18,21] However, the molecular interface between these domains and silica as well as their functional secondary structure when bound to silica is unknown yet.

Biomineral interfaces between biomolecules and silica surfaces were studied by magic-angle spinning nuclear magnetic resonance (MAS NMR) spectroscopy before.[19,22−24] In particular, the backbone conformation of the R5 peptide, coprecipitated with silica, was investigated using MAS NMR techniques.[25] Chemical shift perturbations along the backbone and side chains were linked to respective changes in conformation and proximity of residues to silica.[24−26] Similarly, recent high-resolution MAS NMR studies of enzymes

Received: July 30, 2015
Published: October 9, 2015

DOI: 10.1021/jacs.5b07809
J. Am. Chem. Soc. 2016, 138, 5561−5567

entrapped in porous silica has examined the effects of confinement on the structure and functionality of proteins.[27−30]

In such systems involving peptides bound to silica surfaces, sensitivity and resolution limitations of the NMR technique impede extensive structural characterization of the biomaterial interfaces. Dynamic nuclear polarization (DNP) spectroscopy is becoming widespread as an efficient means of enhancing sensitivity. Through microwave (MW) irradiation of electron spin transitions, polarization is transferred to neighboring nuclei to boost signal-to-noise ratio by 2−3 orders of magnitude. DNP-enhanced MAS NMR measurements were demonstrated on catalytic materials,[31,32] pharmaceutical compounds,[33] organic polymers,[34,35] nanoparticles,[36−39] and functionalized silica.[38,39]

DNP MAS NMR was also implemented for one-dimensional (1D) and two-dimensional (2D) ^{13}C and ^{29}Si measurements in unlabeled samples, relieving the need for elaborate and tedious sample labeling.[40−45] However, rapid deployment of the technique for extensive structural characterization in biological systems is still hampered by low-resolution spectra[46,47] with some exceptions reported.[48−50] The study of functional peptides inside biomaterials is a promising biological setting for DNP employment since line broadening due to trapping of peptides in a wide range of conformations upon cryo-cooling, may occur to a lesser extent since motions are often restricted, a priori, in the confines of a solid material. Yet, no investigations of such systems were reported until now.

In this work, we show that PL12 (KAAKLFKPKASK), a pentalysine peptide derived from Sil3 accelerates silicic acid polymerization into silica in vitro, in a phosphate buffer. We provide snapshots of silica nanoparticle growth by electron microscopy images. The peptide coprecipitates with the silica as it condenses leading to sensitive DNP-enhanced spectra of unlabeled PL12-silica samples at 100 K within minutes without major loss of resolution. We characterize the backbone conformation of PL12 in the PL12-silica complex using DNP-enhanced 2D $^{1}H-^{13}C$ heteronuclear correlation (HETCOR) and 2D ^{13}C double quantum-single quantum (DQ-SQ) MAS NMR measurements and compare it with its solution structure using standard 2D $^{1}H-^{13}C$ heteronuclear multiple quantum coherence (HMQC) and heteronuclear multiple bond coherence (HMBC) measurements and chemical shift perturbation analysis. We also characterize the silica particles formed using ^{29}Si and 2D $^{1}H-^{29}Si$ HETCOR measurements at ambient temperature.

PL12 starts in random coil conformation in solution, with a short β-strand segment around the rigid Pro 8 position. It does not undergo self-assembly prior to addition of the silica precursor even in the presence of the phosphate buffer. Within the silica, the peptide backbone adopts a slightly extended conformation at Phe 6 and a slightly more compact helical structure at Ser 11. Ser 11 has two smaller populations of molecules with its C_β in extended and in random coil conformation, indicating some variability in interaction of its hydroxyl with the silica surface. Proximity of lysine side chains to silica surface is observed through 2D $^{1}H-^{29}Si$ HETCOR experiments. Probing the PL12−silica interface in a high level of detail has ramifications for biomimetic material formation and the ability to follow fine design principles in order to construct materials under ambient conditions with smaller footprint on the environment.

RESULTS AND DISCUSSION

Silica precipitation around PL12 was spontaneous under standard conditions (described in the Experimental Section), as shown by high-resolution scanning electron micrographs (HRSEM) taken during the synthesis (Figure 1). The silica

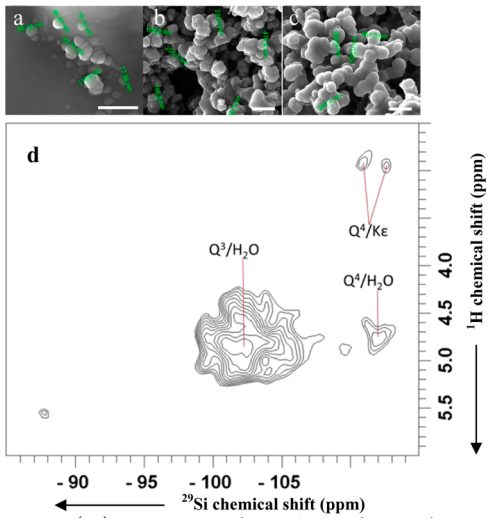

Figure 1. (a−c) HRSEM images of PL12-silica as a function of time. Images (a−c) show the particles formed after 1, 5, and 30 min, respectively. White bar = 300 nm in (a) and 1 μm in (b and c). (d) 2D $^{1}H-^{29}Si$ HETCOR spectrum of PL12-silica recorded using PMLG homonuclear decoupling in t_1, CP contact time of 6 ms, 384 scans, a recycle delay of 3 s, and 208 points in t_1.

precursor, silicic acid, generated in situ by hydrolysis of tetramethyl orthosilicate, was condensed into spherical silica particles that rapidly grew with time. After 1 min, round silica particles precipitated ($d \approx 90$ nm), growing to $d \approx 200$ nm in 5 min and to 500 nm after 30 min. For the silica precipitated without the peptide, growth was slower, showing silica particles of ≈70 nm in an average diameter after 14 min (see HRSEM images in Figure S1). UV absorption measurements of supernatant solution after PL12-silica was spun down indicated that peptide concentration left in solution was negligible (data not shown). PL12-silica particles were washed and analyzed using MAS NMR at room temperature and at 100 K using DNP-enhanced MAS NMR measurements.

The silicon species in the final product were characterized using direct excitation and cross-polarization ^{29}Si MAS NMR experiments (Figure S2). Typical Q^4, Q^3, and Q^2 bands in silica (where Q^n represents known silicon species of the form Si-$(OSi)_nOH_{4-n}$) were observed in the spectra at −112 ppm, −102 ppm, and −92 ppm, respectively. The Q^3/Q^4 ratio extracted from the direct excitation spectrum is comparable to ratios measured in silica from the diatom cell wall (see Table S1), reflecting similar relative content of Si-$(OSi)_3OH$/Si-$(OSi)_4$ groups to biogenic silica.[45,52]

To examine proton-silicon proximities, 2D $^{1}H-^{29}Si$ HETCOR spectra with ^{1}H homonuclear decoupling in t_1 were collected (a representative spectrum is shown in Figure 1). The magnetization transfer from water to Q^3 silicon species is the strongest cross peak in the spectrum (4.85 ppm, −102 ppm), manifesting the presence of strongly bound water near surface Q^3 species. Additional cross peaks of water protons with Q^4 silicon species are also seen. In addition, two cross peaks

DOI: 10.1021/jacs.5b07809
J. Am. Chem. Soc. 2016, 138, 5561−5567

with a ^{1}H chemical shift of 2.9 ppm and ^{29}Si shifts of −111 and −112 ppm were observed. These peaks are assigned to lysine H_{ε} protons in contact with Q^4 silicon sites, indicating close interaction of lysine side chains with silica surface species. The possible association of these cross peaks with exchangeable silanol−water protons on the silica surface[53−56] is overruled because these protons would polarize mainly directly bound silicon species (i.e., Q^3 species at −102 ppm). Moreover, ^{1}H−^{29}Si HETCOR spectra of silica prepared without PL12 (data not shown) show no such cross peaks at 2.9 ppm, confirming that these peaks represent magnetization transfer from peptide protons to the silica. Similar interactions between glycine CH_2 protons (adjacent to amine) and Q^4 sites in silica[51] and between lysine residues in intact *T. pseudonana* and biogenic silica formed[24] were reported before.

Solution NMR ^{13}C spectra of PL12 in water and in phosphate buffer (Figure S3) indicate no conformational change with the addition of phosphate ions. Diffusion NMR measurements of PL12 in phosphate buffer (Figure S4) gave similar peptide diffusivity as in water showing that the peptide does not preassemble prior to silicification unlike R5 peptide,[17,20] other peptides,[25,57] and the whole silaffin from *C. fusiformis*.[19] Contrary to the intact protein, PL12 has no hydrophobic domain and presence of free phosphate ions may not suffice to promote preassembly prior to polymerization.

2D ^{1}H−^{13}C HMQC (Figure 2 and Figure S5) and 2D ^{1}H−^{13}C HMBC (Figure S6) spectra of PL12 were used to assign peaks of different residues in the peptide. The L5, F6, P8, A10, and S11 residues in the peptide were assigned using the two spectra. The two contiguous alanine (A2 and A3) are distinguishable from A10 but not between themselves. The two lysine residues adjacent to the proline (K7, K9) are separated in the spectrum from the three other lysines (K2, K3, and K12) in their C_{α} region, as shown in Figure S5. Peak assignments shown in Figure 2 include annotation of ambiguous lysines as K(X) where X is the index of K position in PL12 (x = 1,4,7,9,12) and the two unresolved alanines as A2(3). A summary of assigned ^{1}H and ^{13}C chemical shifts is given in Table S2. On the basis of chemical shift analysis, the peptide is mostly unstructured. P8 is in a β-strand conformation and its adjacent K7, K9, and A10 residues are in slightly extended conformation. All other residues adopt a random coil conformation. P8 C_{δ},H_{δ} and S11 C_{β},H_{β} cross peaks are doubled suggesting two PL12 conformers exist with subtle backbone differences.

The room temperature ^{13}C cross-polarization (CP) spectrum of PL12-silica acquired using 12288 scans is shown in Figure 3a.

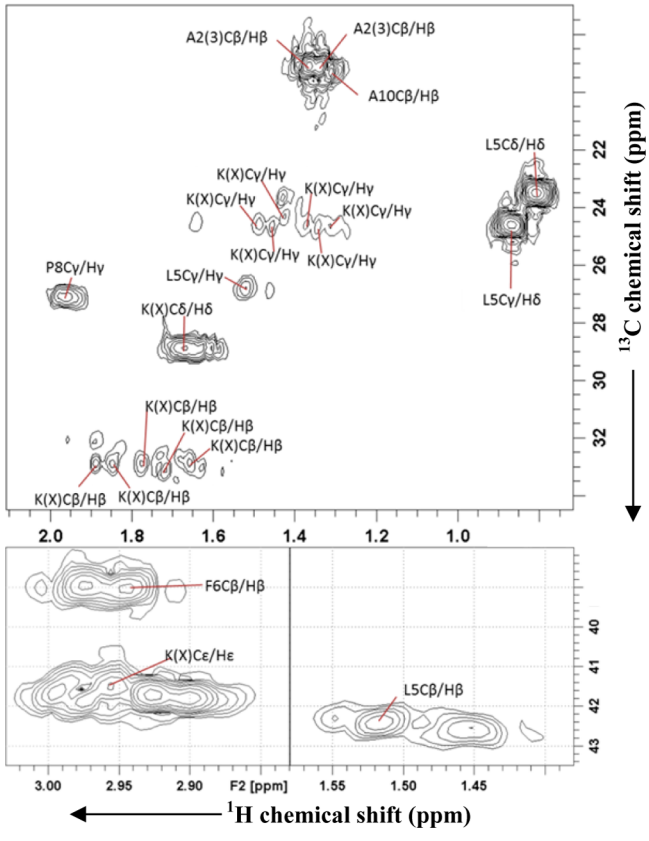

Figure 2. (top) 2D ^{1}H−^{13}C HMQC spectrum of PL12 in solution (high field section) with some of the assigned one- and two-bond coupled carbon−proton peaks annotated. Residues A2 and A3 cannot be distinguished as well as the K residues. (bottom left) K $C_{\varepsilon}H_{\varepsilon}$ and F $C_{\beta}H_{\beta}$ cross peak region. (bottom right) L $C_{\beta}H_{\beta}$ cross peak region.

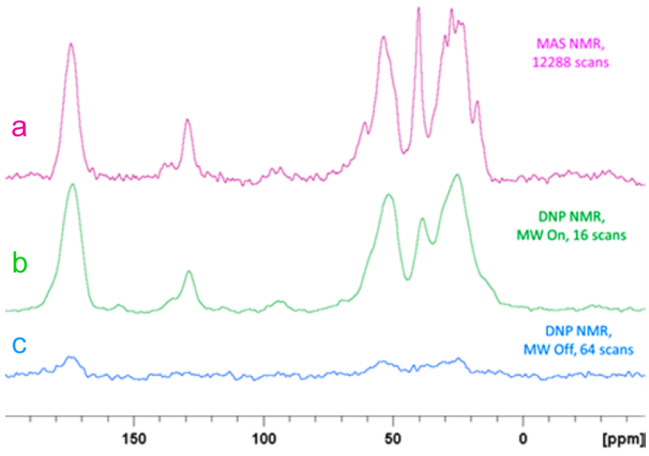

Figure 3. ^{13}C CPMAS spectra of PL12-silica. (a) Spectrum recorded at room temperature using 12288 scans and a recycle delay of 5 s. (b) DNP-enhanced spectrum recorded at 100 K in a fraction of the time (MW irradiation on). (c) Reference spectrum recorded at 100 K without MW irradiation. Low-temperature spectra were recorded with a recycle delay of 1 s.

To speed-up signal accumulation, AMUPOL in phosphate buffer was added to PL12-silica and the sample was cooled to 100 K. DNP-enhanced ^{13}C CPMAS spectra were then taken with MW on and MW off as shown in Figure 3. The DNP-enhanced spectrum showed 30-fold sensitivity increase compared to the MW off spectrum at 100 K, reducing the experimental time down to 64 s with some loss of resolution. The broader lines observed in the 1D ^{13}C DNP-enhanced MAS NMR spectrum are the result of measurements at low temperatures of 100 K, where protein dynamics slows down, resulting in a broader spectral signal.[58] The use of a low amount of AMUPOL (10 mM) ensures that broadening due to paramagnetic relaxation, which typically occurs above 30−40 mM for this radical, is avoided.[58]

2D NMR spectra of the peptide in PL12-silica could then be recorded without the need for isotope enrichment. 2D DNP-enhanced ^{1}H−^{13}C HETCOR MAS NMR spectrum, using DUMBO homonuclear decoupling during ^{1}H evolution, were recorded in less than 2 h (Figure 4, top), providing with

DOI: 10.1021/jacs.5b07809
J. Am. Chem. Soc. 2016, 138, 5561−5567

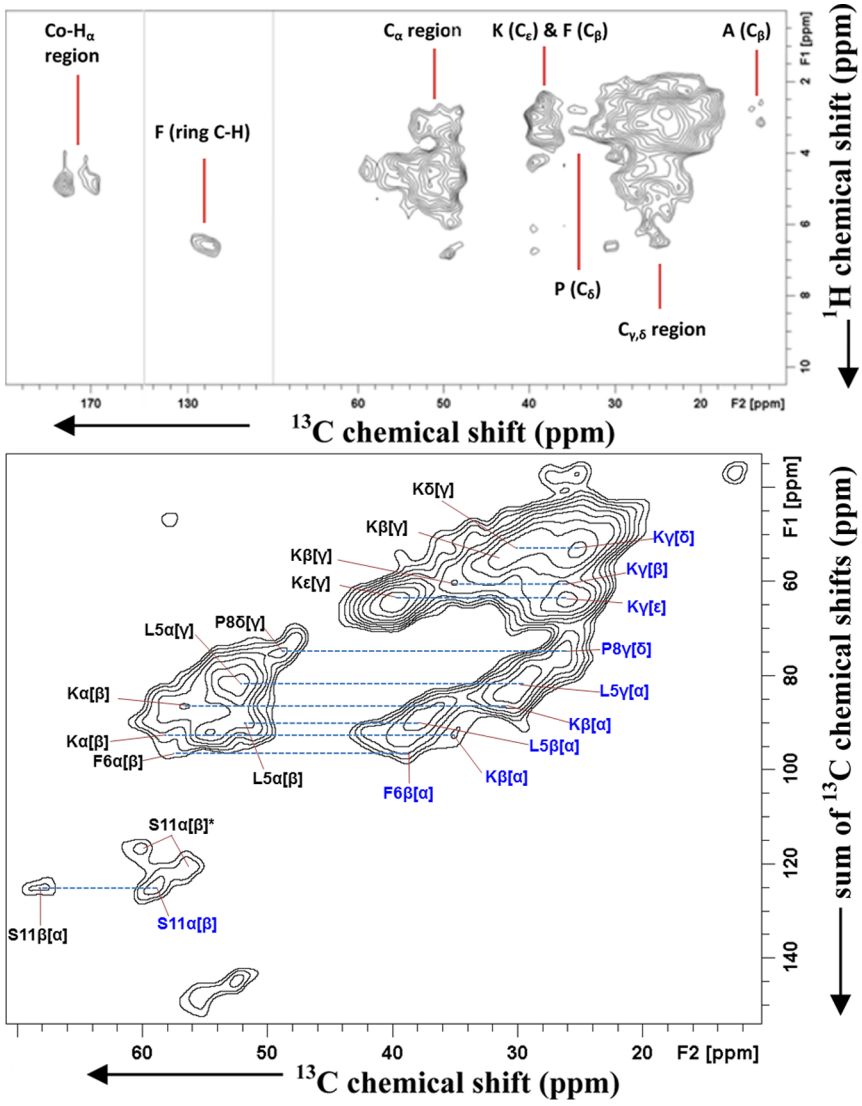

Figure 4. (top) DNP-enhanced 2D $^{1}H-^{13}C$ HETCOR spectra of PL12-silica recorded using DUMBO homonuclear decoupling in t_1 with a contact time of 0.4 ms. (bottom) DNP-enhanced 2D DQ-SQ ^{13}C NMR spectrum of silica-PL12 recorded at 100 K using the SPC5 recoupling sequence for DQ excitation and reconversion. Assigned peaks in the spectrum are annotated in black and cross peaks from coupled carbon annotated in blue and connected with dashed line.

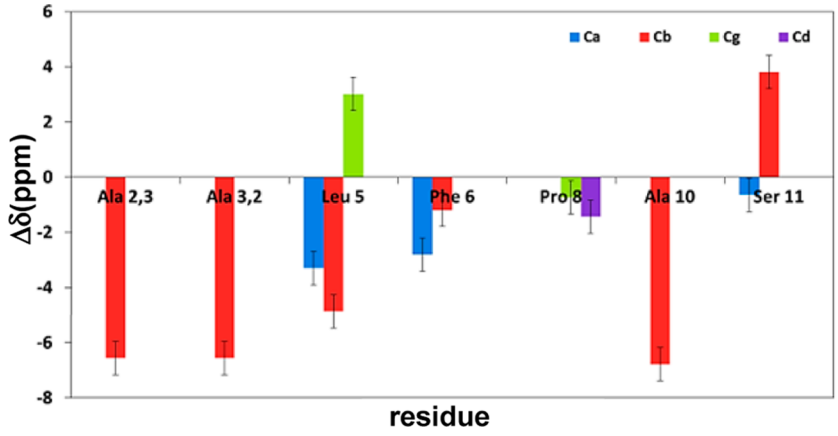

Figure 5. Chemical shift differences for the different carbons in PL12 between its silica bound state and its free state in solution (bound minus free). For Ser 11, the value for the largest population is given in the chart.

moderate resolution and permitting identification of some resonances. At the short CP contact time used (0.4 ms), carbonyl carbons are barely polarized by protons, showing carbonyls involved in strong ^{1}H coupling. Aromatic carbons in

DOI: 10.1021/jacs.5b07809
J. Am. Chem. Soc. 2016, 138, 5561−5567

F6 (128.0 ppm), C_β carbons in alanine (13.5, 14.5 ppm), and the C_δ carbon in P8 (35.0 ppm) are resolved.

DNP-enhanced 2D ^{13}C DQ-SQ NMR measurements[59,60] of silica-PL12 (Figure 4) gave relatively narrow cross peaks between directly bound carbons and enable assignment of most carbons in L5, F6, P8, and S11 carbons as shown in the figure and in Table S3. The chemical shift differences between free and silica-embedded states are summarized in the chart at the bottom of Figure 5. The lysines and alanines could not be uniquely assigned and thus their cross peaks are annotated in the spectrum without their index along the sequence. S11 exhibits a strong $C_{\beta+\alpha}$-C_α peak and two extra weaker peaks (annotated with *) with their C_β shifted upfield by ∼2 and ∼7 ppm relative to the main cross peak. The majority of PL12 molecules have their S11 amino acid in a random coil with slightly more extended character than in solution, and two smaller populations with α-helical and β-strand conformation on this position. This conformational multiplicity may result from the OH group having different H-bonding with silica,[61−63] consequently causing local perturbations to the backbone structure.

In addition, some of the Ala residues acquire a major upfield shift of the C_β carbon (∼6.6 ppm). L5 C_α and C_β carbons are also shifted upfield (∼4−5 ppm), while the C_γ is shifted downfield (∼3 ppm), which may indicate involvement of the specific side chains in interactions with neighboring peptide molecules to form clusters inside the silica. Previous studies of LK and R5 peptide molecules embedded in silica[25,26] have linked similar shifts to the additional shielding by neighboring hydrophobic side chains [e.g., Leu 12 in the LK peptide tetramer (found slightly outside the hydrophobic core) and Ile 18 in the R5 peptide].

CONCLUSIONS

In summary, we demonstrated here the effect of PL12 on silica precipitation under standard conditions and the importance and applicability of DNP MAS NMR for analyzing the structure of peptides in complex heterogeneous states encountered in biomineralization systems. Spontaneous silica precipitation in phosphate buffer was expedited by PL12, and growth of larger spherical biomimetic silica nanoparticles was observed. A backbone conformation change inside the silica was observed for the peptide using 2D DNP MAS NMR without isotope labeling.

Moreover, diffusion NMR measurements showed that no preassembly of the peptide in solution occurs, as suggested for R5 in a recent work.[64] 2D $^1H-^{29}Si$ HETCOR MAS NMR suggest proximity of lysine residues to the Q^4 sites in the silica. These results provide further insights into the role of pentalysine segments in silaffins activity as silica precipitating enzymes and demonstrate that with signal enhancements and reasonable line widths, achieved through DNP NMR, structural studies of biomineral interfaces are facilitated markedly.

EXPERIMENTAL SECTION

Peptide Synthesis. PL12 was synthesized using Fmoc chemistry on a Wang resin in a Protein Technologies PS3 solid phase peptide synthesizer (SPPS). Amino acids were purchased from GL Biochem. After cleavage and lyophilization, the peptide was purified over a C4 column from Grace using a Waters HPLC system and purity >98% was confirmed on a MALDI-TOF mass spectrometer (see Figure S7).

Silica Precipitation in the Presence of the Peptide. Twenty milligrams of the PL12 peptide were dissolved in 7.8 mL of aqueous solution of potassium phosphate buffer (50 mM), pH = 7, to a final concentration of 2 mM. In a separate vessel, 0.15 mL tetramethoxysilane (TMOS) was dissolved in 0.85 mL of HCl (1 mM) (final concentration of 1.01 M) and stirred for 4 min. 0.62 mL of Silicic acid solution, which had formed from the TMOS, was added to the peptide solution. The mixture was stirred for 30 min, centrifuged for another 30 min, and then washed with double-distilled water. The precipitate was dried at 30 °C for 3 days. To follow the reaction, samples were taken throughout the process and placed on carbon tape for high-resolution scanning electron microscopy (HRSEM) measurements. No traces of TMOS were found in the ^{29}Si spectrum at the −78.5 ppm line, indicating complete conversion of the precursor TMOS to silica.

High-Resolution Scanning Electron Microscopy. All measurements were carried out on a FEI Magellan 400L microscope. The samples were imaged at an accelerating voltage of 15 kV. Images were collected at several time intervals to monitor the silica condensation and particle growth process.

Solid State MAS NMR. NMR measurements were performed on a Bruker 11.7T Avance III spectrometer equipped with a 4 mm VTN CPMAS probe at a spinning rate of 10 kHz. $^1H-^{13}C$ and $^1H-^{29}Si$ CP experiments employed a ^1H 90° pulse of 2.5 μs, followed by CP transfer using a ramped field on ^1H (39.3 to 78.6 kHz), a 49.0 kHz field on ^{13}C, and a 49.9 kHz field on ^{29}Si separately and composite-pulse ^1H decoupling using the SPINAL64 sequence with RF field of 95.1 kHz during acquisition. $^1H-^{13}C$ CPMAS spectrum was collected with 12288 scans and recycle delay of 5 s, and $^1H-^{29}Si$ CPMAS spectrum was collected with 49152 scans and recycle delay of 2 s. 1D ^{29}Si direct polarization measurements were acquired using a 4.6 μs ^{29}Si 90° pulse, 4912 scans, and a recycle delay of 30 s. ^{29}Si 1D spectra were analyzed using the DMFIT program by Massiot et al.[65] The 2D $^1H-^{29}Si$ heteronuclear correlation spectrum was collected using homonuclear decoupling in t_1, at an effective field of 92.6 kHz with the phase modulated Lee−Goldburg (PMLG) sequence, followed by CP irradiation for 6.0 ms using similar fields on ^1H and ^{29}Si as in the 1D $^1H-^{29}Si$ CP experiments and SPINAL64 heteronuclear decoupling during acquisition with RF field of 95.1 kHz.

Solid State DNP MAS NMR. DNP NMR measurements were carried out on 400 MHz Bruker Avance III spectrometer equipped with a 263 GHz gyrotron and a cryogenic triple-resonance 3.2 mm MAS probe at a spinning rate of 8 kHz and temperature of 100 K at the FMP institute in Berlin. 30 μL of 10 mM AMUPol was added to 30 mg of the PL12-silica sample and packed into a 3.2 mm rotor. DNP-enhanced 1D ^{13}C NMR measurements were carried out using a ^1H 90° pulse of 3.0 μs, followed by a CP contact time of 2 ms using ramped field on ^1H (39.3 to 78.6 kHz) and 49.0 kHz field on ^{13}C and a composite-pulse ^1H decoupling using the TPPM sequence at 83 kHz during acquisition, a spinning rate of 8 kHz, and a recycle delay of 1 s. DNP-enhanced 2D $^1H-^{13}C$ heteronuclear correlation spectra were collected using DUMBO homonuclear decoupling scheme at an effective field of 77 kHz, followed by CP irradiation using similar fields on ^1H and ^{13}C as in the 1D $^1H-^{13}C$ CP experiments for 0.4 and 2 ms. In total, 160 t_1 points and 4 repetitions were collected per experiment using similar ^1H decoupling and recycle delay values as in the 1D $^1H-^{13}C$ CP experiments. DNP-enhanced 2D ^{13}C DQ-SQ measurements were carried out using 160 t_1 points, 128 repetitions, 8 kHz spinning, and a recycle delay of 0.5 s. A narrowband DQ excitation period employing the $SPC5_3$ pulse train and a similar DQ-SQ reconversion period using the same pulse train was employed. Field strength of 26.7 kHz was used on ^{13}C during the SPC5 periods. ^1H LG decoupling during SPC5 excitation and reconversion periods was carried out at a B_1 field of 83 kHz. The excitation and reconversion times were selected for one/two-bond correlations, at most.

Solution NMR. NMR measurements were performed on a Bruker 16.4 T Avance III spectrometer equipped with a cryogenic TCI probe with z axis gradients. All experiments were conducted on 4.5 mM PL12 in 0.5 mL of solvent. ^{13}C direct polarization spectra were collected with 30000 scans and recycle delay of 0.3 ms. 2D $^1H-^{13}C$ heteronuclear multiple quantum coherence (HMQC) and heteronuclear multiple bond coherence (HMBC) spectra were collected

DOI: 10.1021/jacs.5b07809
J. Am. Chem. Soc. 2016, 138, 5561−5567

using smoothed square gradient (SMSQ) pulses. Data were acquired in 72 scans, with a recycle delay of 1 s. Diffusion NMR measurements were performed using the pulsed-field echo with a recycle delay of 6.6 s.

■ ASSOCIATED CONTENT

Supporting Information

The Supporting Information is available free of charge on the ACS Publications website at DOI: 10.1021/jacs.5b07809.

HRSEM images of silica precipitated without PL12, ^{29}Si CPMAS and direct polarization spectra of PL12-silica with peak deconvolution, ^{13}C direct polarization liquid NMR spectra of PL12 in phosphate buffer and in aqueous solution, ^{1}H diffusion NMR results, 2D ^{1}H−^{13}C HMQC and 2D ^{1}H−^{13}C HMBC of PL12 in aqueous solution, mass spectrometry data, table of Q^3/Q^4 ratios in PL12-silica and various biogenic silica, and tables of assigned ^{1}H and ^{13}C peaks of PL12 in solution and assigned ^{13}C peaks of PL12-silica in the solid state (PDF)

■ AUTHOR INFORMATION

Corresponding Author

*gil.goobes@biu.ac.il.

Present Addresses

§Aarhus Institute of Advanced Studies (AIAS), Aarhus University, Høegh-Guldbergs Gade 6B, 8000, Aarhus C, Denmark.

⊥Interdisciplinary Nanoscience Center (iNANO), Aarhus University Gustav Wieds Vej 14, 8000, Aarhus C, Denmark.

Author Contributions

The manuscript was written through contributions of all authors. All authors have given approval to the final version of the manuscript.

Notes

The authors declare no competing financial interest.

■ ACKNOWLEDGMENTS

The authors thank Ido Fuchs from the chemistry department at Bar-Ilan University for his help with the HRSEM measurements.

■ REFERENCES

(1) Hildebrand, M.; Holton, G.; Joy, D. C.; Doktycz, M. J.; Allison, D. P. *J. Microsc.* **2009**, *235*, 172−187.

(2) Kröger, N.; Poulsen, N. *Annu. Rev. Genet.* **2008**, *42*, 83−107.

(3) Fang, Y.; Wu, Q.; Dickerson, M. B.; Cai, Y.; Shian, S.; Berrigan, J. D.; Poulsen, N.; Kroger, N.; Sandhage, K. H. *Chem. Mater.* **2009**, *21*, 5704−5710.

(4) Lee, S. J.; Huang, C. H.; Shian, S.; Sandhage, K. H. *J. Am. Ceram. Soc.* **2007**, *90*, 1632−1636.

(5) Bao, Z.; Weatherspoon, M. R.; Shian, S.; Cai, Y.; Graham, P. D.; Allan, S. M.; Ahmad, G.; Dickerson, M. B.; Church, B. C.; Kang, Z.; Abernathy, H. W., III; Summers, C. J.; Liu, M.; Sandhage, K. H. *Nature* **2007**, *446*, 172−175.

(6) Payne, E. K.; Rosi, N. L.; Xue, C.; Mirkin, C. A. *Angew. Chem., Int. Ed.* **2005**, *44*, 5064−5067.

(7) Coradin, T.; Lopez, P. J. *ChemBioChem* **2003**, *4*, 251−259.

(8) Foo, C. W.; Huang, J.; Kaplan, D. L. *Trends Biotechnol.* **2004**, *22*, 577−585.

(9) Naik, R.; Stone, O. *Mater. Today* **2005**, *8*, 18−26.

(10) Vrieling, E. G.; Hazelaar, S.; Gieskes, W. W.; Sun, Q.; Beelen, T. P.; Van Santen, R. A. *Progress in Molecular and Subcellular Biology*; Progress in Molecular and Subcellular Biology; Springer: Berlin, 2003; Vol. 33, pp 301−334.

(11) Sumper, M. *Science* **2002**, *295*, 2430−2433.

(12) Kroger, N.; Sandhage, K. H. *MRS Bull.* **2010**, *35*, 122−126.

(13) Poulsen, N.; Scheffel, A.; Sheppard, V. C.; Chesley, P. M.; Kröger, N. *J. Biol. Chem.* **2013**, *288*, 20100−20109.

(14) Kröger, N.; Deutzmann, R.; Sumper, M. *Science* **1999**, *286*, 1129−1132.

(15) lopez, P. J.; Descles, J.; Allen, A. E.; Bowler, C. *Curr. Opin. Biotechnol.* **2005**, *16*, 180−186.

(16) Wieneke, R.; Bernecker, A.; Riedel, R.; Sumper, M.; Steinem, C.; Geyer, A. *Org. Biomol. Chem.* **2011**, *9*, 5482−5486.

(17) Knecht, M. R.; Wright, D. W. *Chem. Commun.* **2003**, *24*, 3038−3039.

(18) Belton, D.; Paine, G.; Patwardhan, S. V.; Perry, C. C. *J. Mater. Chem.* **2004**, *14*, 2231−2241.

(19) Kröger, N.; Lorenz, S.; Brunner, E.; Sumper, M. *Science* **2002**, *298*, 584−586.

(20) Lechner, C. C.; Becker, C. F. W. *J. Pept. Sci.* **2014**, *20*, 152−158.

(21) Brunner, E.; Richthammer, P.; Ehrlich, H.; Paasch, S.; Simon, P.; Ueberlein, S.; van Pée, K. H. *Angew. Chem., Int. Ed.* **2009**, *48*, 9724−9727.

(22) Patwardhan, S. V.; Emami, F. S.; Berry, R. J.; Jones, S. E.; Naik, R. R.; Deschaume, O.; Heinz, H.; Perry, C. C. *J. Am. Chem. Soc.* **2012**, *134*, 6244−6256.

(23) Christiansen, S. C.; Hedin, N.; Epping, J. D.; Janicke, M. T.; del Amo, Y.; Demarest, M.; Brzezinski, M.; Chmelka, B. F. *Solid State Nucl. Magn. Reson.* **2006**, *29*, 170−182.

(24) Wisser, D.; Brückner, S. I.; Wisser, F. M.; Althoff-Ospelt, G.; Getzschmann, J.; Kaskel, S.; Brunner, E. *Solid State Nucl. Magn. Reson.* **2015**, *66-67*, 33−39.

(25) Roehrich, A.; Drobny, G. *Acc. Chem. Res.* **2013**, *46*, 2136−2144.

(26) Zane, A. C.; Michelet, C.; Roehrich, A.; Emani, P. S.; Drobny, G. P. *Langmuir* **2014**, *30*, 7152−7161.

(27) Mirau, P. A.; Serres, J. L.; Lyons, M. *Chem. Mater.* **2008**, *20*, 2218−2223.

(28) Song, X.; Jiang, Z.; Li, L.; Wu, H. *Front. Chem. Sci. Eng.* **2014**, *8*, 353−361.

(29) Ravera, E.; Schubeis, T.; Martelli, T.; Fragai, M.; Parigi, G.; Luchinat, C. *J. Magn. Reson.* **2015**, *253*, 60−70.

(30) Fragai, M.; Luchinat, C.; Martelli, T.; Ravera, E.; Sagi, I.; Solomonov, I.; Udi, Y. *Chem. Commun.* **2014**, *50*, 421−423.

(31) Vitzthum, V.; Miéville, P.; Carnevale, D.; Caporini, M. A.; Gajan, D.; Copéret, C.; Lelli, M.; Zagdoun, A.; Rossini, A. J.; Lesage, A.; Emsley, L.; Bodenhausen, G. *Chem. Commun.* **2012**, *48*, 1988−1990.

(32) Samantaray, M. K.; Alauzun, J.; Gajan, D.; Kavitake, S.; Mehdi, A.; Veyre, L.; Lelli, M.; Lesage, A.; Emsley, L.; Coperet, C.; Thieuleux, C. *J. Am. Chem. Soc.* **2013**, *135*, 3193−3199.

(33) Linden, A. H.; Lange, S.; Franks, W. T.; Akbey, U.; Specker, E.; van Rossum, B. J.; Oschkinat, H. *J. Am. Chem. Soc.* **2011**, *133*, 19266−19269.

(34) Blanc, F.; Chong, S. Y.; McDonald, T. O.; Adams, D. J.; Pawsey, S.; Caporini, M. A.; Cooper, A. I. *J. Am. Chem. Soc.* **2013**, *135*, 15290−15293.

(35) Ouari, O.; Phan, T.; Ziarelli, F.; Casano, G.; Aussenac, F.; Thureau, P.; Gigmes, D.; Tordo, P.; Viel, S. *ACS Macro Lett.* **2013**, *2*, 715−719.

(36) Lafon, O.; Thankamony, A. S. L.; Rosay, M.; Aussenac, F.; Lu, X.; Trébosc, J.; Bout-Roumazeilles, V.; Vezin, H.; Amoureux, J. P. *Chem. Commun.* **2013**, *49*, 2864−2866.

(37) Lafon, O.; Thankamony, A. S. L.; Kobayashi, T.; Carnevale, D.; Vitzthum, V.; Slowing, I. I.; Kandel, K.; Vezin, H.; Amoureux, J. P.; Bodenhausen, G.; Pruski, M. *J. Phys. Chem. C* **2013**, *117*, 1375−1382.

(38) Ravera, E.; Michaelis, V. K.; Ong, T. C.; Keeler, E. G.; Martelli, T.; Fragai, M.; Griffin, R. G.; Luchinat, C. *ChemPhysChem* **2015**, *16*, 2751−2754.

(39) Akbey, Ü.; Altin, B.; Linden, A.; Özçelik, S.; Gradzielski, M.; Oschkinat, H. *Phys. Chem. Chem. Phys.* **2013**, *15*, 20706−20716.

(40) Lelli, M.; Gajan, D.; Lesage, A.; Caporini, M. A.; Vitzthum, V.; Mieville, P.; Heroguel, F.; Rascon, F.; Roussey, A.; Thieuleux, C.;

DOI: 10.1021/jacs.5b07809
J. Am. Chem. Soc. 2016, 138, 5561−5567

Boualleg, M.; Veyre, L.; Bodenhausen, G.; Coperet, C.; Emsley, L. *J. Am. Chem. Soc.* **2011**, *133*, 2104−2107.
(41) Corzilius, B.; Michaelis, V. K.; Penzel, S. A.; Ravera, E.; Smith, A. A.; Luchinat, C.; Griffin, R. G. *J. Am. Chem. Soc.* **2014**, *136*, 11716−11727.
(42) Lesage, A.; Lelli, M.; Gajan, D.; Caporini, M. A.; Vitzthum, V.; Mieville, P.; Alauzun, J.; Roussey, A.; Thieuleux, C.; Mehdi, A.; Bodenhausen, G.; Coperet, C.; Emsley, L. *J. Am. Chem. Soc.* **2010**, *132*, 15459−15461.
(43) Vitzthum, V.; Borcard, F.; Jannin, S.; Morin, M.; Miéville, P.; Caporini, M. A.; Sienkiewicz, A.; Gerber-Lemaire, S.; Bodenhausen, G. *ChemPhysChem* **2011**, *12*, 2929−2932.
(44) Lafon, O.; Rosay, M.; Aussenac, F.; Lu, X.; Trebosc, J.; Cristini, O.; Kinowski, C.; Touati, N.; Vezin, H.; Amoureux, J. P. *Angew. Chem., Int. Ed.* **2011**, *50*, 8367−8370.
(45) Lee, D.; Monin, G.; Duong, N. T.; Lopez, I. Z.; Bardet, M.; Mareau, V.; Gonon, L.; De Paepe, G. *J. Am. Chem. Soc.* **2014**, *136*, 13781−13788.
(46) Hall, D. A. D.; Gerfen, G. L.; Inati, S. J.; Becerra, L. R.; Dahlquist, F. W.; Griffin, R. G. *Science* **1997**, *276*, 930−932.
(47) Rosay, M.; Lansing, J. C.; Haddad, K. C.; Bachovchin, W. W.; Herzfeld, J.; Temkin, R. J.; Griffin, R. G. *J. Am. Chem. Soc.* **2003**, *125*, 13626.
(48) Bajaj, V. S.; Mak-Jurkauskas, M. L.; Belenky, M.; Herzfeld, J.; Griffin, R. G. *Proc. Natl. Acad. Sci. U. S. A.* **2009**, *106*, 9244.
(49) Debelouchina, G. T.; Bayro, M. J.; Fitzpatrick, A. W.; Ladizhansky, V.; Colvin, M. T.; Caporini, M. A.; Jaroniec, C. P.; Bajaj, V. S.; Rosay, M.; MacPhee, C. E.; Vendruscolo, M.; Maas, W. E.; Dobson, C. M.; Griffin, R. G. *J. Am. Chem. Soc.* **2013**, *135*, 19237−19247.
(50) Takahashi, H.; Ayala, I.; Bardet, M.; De Paepe, G.; Simorre, J. P.; Hediger, S. *J. Am. Chem. Soc.* **2013**, *135*, 5105−5110.
(51) Ben Shir, I.; Kababya, S.; Schmidt, A. *J. Phys. Chem. C* **2012**, *116*, 9691−9702.
(52) Bertermann, R.; Kröger, N.; Tacke, R. *Anal. Bioanal. Chem.* **2003**, *375*, 630−634.
(53) Lutz, K.; Gröger, C.; Sumper, M.; Brunner, E. *Phys. Chem. Chem. Phys.* **2005**, *7*, 2812−2815.
(54) Trebosc, J.; Wiench, J. W.; Huh, S.; Lin, V. S. Y.; Pruski, M. *J. Am. Chem. Soc.* **2005**, *127*, 7587−7593.
(55) Trebosc, J.; Wiench, J. W.; Huh, S.; Lin, V. S. I.; Pruski, M. *J. Am. Chem. Soc.* **2005**, *127*, 3057−3068.
(56) L'Espinose de la Caillerie, J. B.; Aimeur, M. R.; El Kortobi, Y.; Legrand, A. P. J. *J. Colloid Interface Sci.* **1997**, *194*, 434−439.
(57) Patwardhan, S. V.; Maheshwari, R.; Mukherjee, N.; Kiick, K. L.; Clarson, S. J. *Biomacromolecules* **2006**, *7*, 491−497.
(58) Linden, A. H.; Franks, W. T.; Akbey, Ü.; Lange, S.; van Rossum, B. J.; Oschkinat, H. *J. Biomol. NMR* **2011**, *51*, 283−292.
(59) Hohwy, M.; Rienstra, C. M.; Jaroniec, C. P.; Griffin, R. G. *J. Chem. Phys.* **1999**, *110*, 7983−7992.
(60) Takahashi, H.; Lee, D.; Dubois, L.; Bardet, M.; Hediger, S.; De Paëpe, G. *Angew. Chem.* **2012**, *124*, 11936−11939.
(61) Yokoi, T.; Seo, S.; Chino, N.; Shimojima, A.; Okubo, T. *Microporous Mesoporous Mater.* **2009**, *124*, 123−130.
(62) Srinivasan, G.; Sander, L. C.; Müller, K. *Anal. Bioanal. Chem.* **2005**, *384*, 514−524.
(63) Ossenkamp, G. C.; Kemmitt, T.; Johnston, J. H. *Chem. Mater.* **2001**, *13*, 3975−3980.
(64) Senior, L.; Crump, M. P.; Williams, C.; Booth, P. J.; Mann, S.; Perriman, A. W.; Curnow, P. *J. Mater. Chem. B* **2015**, *3*, 2607−2614.
(65) Massiot, D.; Fayon, F.; Capron, M.; King, I.; Le Calve, S.; Alonso, A.; Durand, J. O.; Bujoli, B.; Gan, Z.; Hoatson, G. *Magn. Reson. Chem.* **2002**, *40*, 70−76.

DOI: 10.1021/jacs.5b07809
J. Am. Chem. Soc. 2016, 138, 5561−5567